63-1-3

AIR FORCE INSTITUTE OF TECHNOLOGY

AIR UNIVERSITY
UNITED STATES AIR FORCE

SCHOOL OF ENGINEERING

WRIGHT-PATTERSON AIR FORCE BASE, OHIO

AF-WP-O-MAY 62 3,500

The Effect of Two MEV Deuteron And Proton Radiation on the Conductivity In N-Type Germanium Dendrite Crystals

Capt Ralph H. Jacobson

GA/Phys/62-9

THE EFFECT OF TWO MEV DEUTERON AND PROTON RADIATION ON THE CONDUCTIVITY IN N-TYPE GERMANIUM DENDRITE CRYSTALS

THESIS

Presented to the Faculty of the School of Engineering

of the Air Force Institute of Technology

Air University

in Partial Fulfillment of the

Requirements for the Degree of

Master of Science

By

Ralph H. Jacobson, B. S.

Capt USAF

Graduate Astronautics

August 1962

Preface

The value of this investigation is not, in my opinion, any information gained as the result of the experiment. Rather, the value is the opportunity afforded me to work independently on a project in a laboratory. I am sure the experience will be of value to me in any future technical assignment I may receive.

I want to thank the many people who helped me during this investigation: Dr. William Lehmann for his guidance; Dr. Gale Harris and Mr. David Breitenbecker for the many hours they freely gave at night and on weekends helping me with the Van de Graaf; Capt. James Diebold for the apparatus I used, and the many helpful hints he gave; all the technicians in the AFIT physics laboratory who were never too busy to listen to my problems and try to help me; and finally to my wife and family for their understanding attitude.

Contents

List of Figures

GA/Phys/62-9

Abstract

N-type germanium crystals, both dendrites and ordinary crystals, were irradiated with two MEV deuterons and protons in order to find if any differences in the effects on conductivity of radiation exist between the two types of crystals. The electron reduction rate and the hole production rate was found to be greater by a factor of approximately two in the dendrite crystals. The results indicate the formation of acceptor levels associated with the surface. These levels are relatively more important in the more perfect surfaces of the dendrites. A demonstration, showing the possibility of making electronic devices by a simple radiation process, was also conducted.

GA/Phys/62-9

THE EFFECT OF TWO MEV DEUTERON AND PROTON RADIATION ON THE CONDUCTIVITY IN N-TYPE GERMANIUM DENDRITE CRYSTALS

I. Introduction

Dendrite crystals of germanium differ from ordinary single crystals in that they have two surfaces which are naturally smooth. These surfaces are composed of areas of extreme flatness, separated by steps whose height is 600 Å or less. Dendrites have been grown with surfaces showing no discernible steps whatever (Ref 1: 55). The surfaces of dendrites are much smoother than the surfaces of an ordinary crystal which has been chemically etched or mechanically polished. Many previous studies have found that the electrical properties of germanium are dependent on the surface properties of the crystals. If the radiation effects are also dependent on the surface properties of the crystals, then there should be a difference in the electrical properties of dendrites and ordinary single crystals after radiation.

Problem Statement

It is the purpose of this study to determine if there is any difference in the conductivity change of dendrites and ordinary single crystals of germanium during 2 MEV deuteron and proton radiation. Conductivity measurements were made during the radiation from the Aeronautical Research Laboratories' 2 MEV Van de Graaf Accelerator.

Interpreation of the differences in the conductivity measurements appear in the conclusions section.

An unsuccesful attempt was made to measure the lifetime of both kinds of crystals as a function of radiation. The attempt was unsuccessful because of a faulty Kerr cell in the lifetime measuring apparatus. Suggestions for measuring the lifetime during radiation in a later experiment appear in the Appendix.

In addition to the above, the possibility of making electronic devices by a radiation process was demonstrated.

The Experiment

One N-type and two P-type ordinary single crystals, and two N-type dendrites were prepared and subjected to 2 MEV deuteron radiation. Conductivity measurements of the crystals at various levels of radiation were obtained. One N-type dendrite was prepared, and two thin sections were subjected to 2 MEV deuteron radiation. The rest of the crystal was shielded with a copper template. A measurement of electrical current at various voltages was made on the irradiated and shielded parts of the crystal. One N-type dendrite and one N-type ordinary single crystal were prepared and subjected to 2 MEV proton radiation. Conductivity measurements of these two crystals at various levels of radiation were also obtained.

Preliminary Results

The effect of deuteron radiation on the conductivity of N-type

and P-type ordinary single crystals is in general agreement with earlier experiments. There was a definite difference in the effect of radiation on dendrite crystals. The number of carriers removed per incident deuteron was greater by a factor of 2 in the dendrite. The number of carriers induced per incident deuteron after the samples changed to P-type was less by a factor of 2 in the dendrite. However, heating of the ordinary N-type crystal, while being irradiated after the minimum conductivity point had been reached, put the carrier induction rate in doubt.

The number of carriers removed per incident proton was also greater in the dendrite than in the ordinary crystal. The dendrite showed a reduction rate of 1.6 times that of the ordinary crystal. However, the number of carriers induced after the minimum conductivity point had been reached was also greater in the dendrite. The factor here was 1.8.

The measurements made on the dendrite sample which had two thin strips exposed to deuteron radiation demonstrated the possibility of making an electronic device by a radiation process. The two strips acted as rectifiers imbeded in the dendrite crystal. However, more information about the conductivity and lifetime changes during radiation must be obtained before the possibility of making such a device in this way becomes a certainty.

Organization

The remainder of this report is presented as follows:

1. The theory of radiation damage is discussed in Chapter II.

2. The experimental apparatus and proceedures are described in Chapter III.

3. Results of the experiment are presented in Chapter IV.

4. Conclusions based on the results are stated in Chapter V.

5. Suggestions for measuring the lifetime of dendrites after radiation are presented in the Appendix.

II. Theory

Germanium Crystals

Germanium, being a group IV element, has four valence electrons surrounding a stable ionic core. Each of these electrons tends to form a covalent or electron pair bond with another atom. This tendency is completely satisfied in a solid state crystal structure of pure germanium. Each atom shares an electron with four other atoms forming four covalent bonds with its nearest neighbors. Thus, in the perfect germanium crystal at low temperatures, the electrons are tightly bound and unable to enter into the conduction process.

The atoms of a germanium crystal arrange themselves in a diamond structure. The space lattice of germanium is face-centered cubic with a basis of two atoms at 000 and 1/4 1/4 1/4 associated with each lattice point. The lattice constant is 5.62 $\mathring{A}$ (Ref 11:6). This lattice structure is relatively empty. The proportion of the available volume which may be filled by hard spheres is only 0.34. There is ample volume available for an atom to occupy an interstitial position in this crystal structure. Atoms knocked-on by proton or deuteron bombardment can locate in an interstitial position, thereby creating a vacancy interstitial pair or Frenkel defect. These defects can modify the electrical properties of the solid.

Conductivity

As in other semiconductors, conduction in germanium is produced

by destroying the perfection of the valence bond structure. In a perfect crystal, destruction of valence bonds by some means such as thermal agitation, releases electrons that may move under the influence of an electric field. The released electrons leave holes in the valence structure behind. These holes also move under the influence of an electric field, but in the opposite direction. The direction of current flow is the same for both the electrons and the holes, and is the directions the holes move when a field is applied.

According to the theory of quantum-mechanics, a high degree of symmetry exists between conduction with electrons and conduction with holes. There is only a slight difference between these two processes. One may think of a hole moving through a crystal exactly the same way as one thinks of a free electron moving through a crystal except that the sign of the charge is opposite (Ref 11:11). The conductivity is given by

$$\sigma = e(n\mu_e + p\mu_h) \qquad (1)$$

where σ is the conductivity in $(\text{ohm} - \text{cm})^{-1}$

e is the charge of the electron in coulombs

n is the density of electrons in electrons / cm^3

p is the density of holes in holes / cm^3

μ_e and μ_h are the mobilities of electrons and holes, respectively, in cm/sec per volt/cm.

The density of electrons and holes would be very small in

a pure germanium crystal at room temperature. Only those electrons and holes freed by thermal agitation would be available for conduction. In germanium crystal devices small amounts of impurities are added to increase the carrier density. It is believed that each impurity atom displaces one germanium atom from its regular site in the crystal structure. Thus, an impurity atom from Group V of the Periodic Table, such as arsenic, would form four covalent bonds with each of its nearest neighbors and have one electron left over for conduction. An impurity atom from Group III, such as boron, would form three covalent bonds with its nearest neighbors, leaving one bond unformed and creating a hole for conduction. A crystal with Group V, or donor, impurities is an N-type crystal. Group III, or acceptor, impurities create P-type crystals. At room temperature in an N-type crystal, $n >> p$, and p may be taken to be zero in equation (1). The opposite is true of a P-type crystal (Ref 11:16).

Energy Levels and Bands

A definite amount of energy must be given an electron in order to break a covalent bond. It may be shown, quantum mechanically, that the valence electrons of a germanium atom in a crystal exist either in a band of energies called the valence band or in a band of energies called the conduction band as shown in Figure 1. The space between these two energy bands is called the energy gap, and germanium valence electrons may not exist with any value of energy

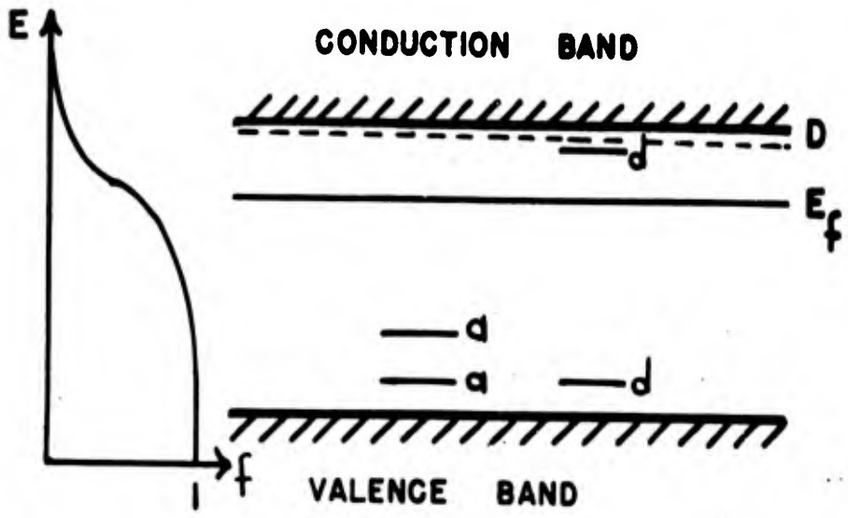

N-TYPE

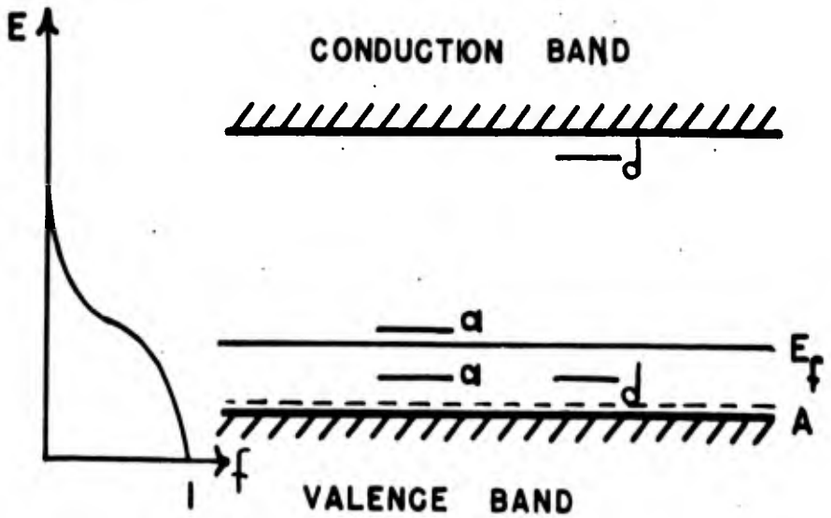

P-TYPE

ENERGY LEVEL DIAGRAMS
(FROM REF 6:166)

FIG. 1

in the gap. In order to break a covalent bond then, at least the energy of the gap must be added to an electron.

Impurities added to germanium give rise to energy levels in the energy gap. The impurity energy levels are labeled, D, for the donor level in N-type and, A, for the acceptor level in P-type in Figure 1. It can be seen that much less energy must be added to an electron having the donor energy level than must be added to an electron in the valence band in order for the electron to gain an energy level in the conduction band. The same is true for a hole with an acceptor energy level and the valence band. The energy gap for germanium is 0.72 EV, and the donor and acceptor levels are approximately 0.04 EV from the conduction band and valence band, respectively. The energies required to remove holes from acceptors and electrons from donors are so small that at room temperature the donors and acceptors are effectively fully ionized (Ref 11:24).

The energy level in Figure 1 labeled E_f is the Fermi level. It is defined by

$$f = \frac{1}{1 + \exp (E - E_f / kT)} \qquad (2)$$

where f is the probability that a quantum state at energy E is occupied.

E_f is the Fermi energy level

k is the Boltzmann constant

T is the absolute temperature

E_f is that energy where f = 1/2.

The function, f, is also plotted in Figure 1. The Fermi level is related to the carrier concentration. As the number of conduction electrons increase, E_f moves toward the conduction band. As the number of holes increase, E_f moves toward the valence band. The effect on the Fermi level of radiation will be covered in the next section.

Radiation Damage

It has been found that radiation causes changes in both the carrier densities, n and p and the mobilities, μ_e and μ_h in (1). However, it has been found that the carrier densities change by orders of magnitude while the mobilities change by a factor of approximately two. The mobilities will be considered constant in this report. Their values will be taken as 3600 and 1700 cm / sec per volt / cm for μ_e and μ_h respectively (Ref 11:17).

Damage in germanium crystals caused by irradiation with energetic charged particles is complex, and no theory exists which can fully predict the change in conductivity during radiation. Radiation damage may be of two kinds. There is damage causing permanent effects and damage causing transient effects. The theory will be divided into these two categories.

Permanent Effects. There are two basic processes by which radiation can produce permanent effects. These processes are

transmutations and atomic displacements. They have in common that the end result is the introduction of new levels into the forbidden energy gap (Ref 8:8). The number of transmutations per incident charged particle is very small. For 10 MEV deuterons the number is on the order of only 5×10^{-4} per deuteron. From earlier experiments, the carriers removed per incident deuteron are 4 or 5 orders of magnitude greater than this; therefore, the effects of transmutations are considered negligible (Ref 7:51-52).

The lattice defect, which results from the displacement of an atom from its original lattice site to an interstitial position, is the source of most permanent radiation effects. Although there are other models (Ref 2:1220), the model of James and Lark-Horovitz is simple, and it satisfactorily explains the energy levels produced by lattice defects. According to the JLH model, displaced atoms cause vacancy-interstitial pairs. Interstitial atoms give donor levels and vacancies give acceptor levels. It is assumed that each type of defect gives two levels. These levels are labeled a and d in Figure 1. Depending on the position of the Fermi Level, these vacancy-interstitial levels may add to, or subtract from the number of carriers. If the donor levels are above E_f, or the acceptor levels below E_f, then changes in the number of carriers will occur. Adding acceptor levels below E_f reduces the concentration of conduction electrons in N-type and increases the hole con-

centration in P-type crystals (Ref 6:166).

The number of displaced atoms per incident charged particle is one of the few quantitative predictions which present theory can make. An incident charged particle transfers energy directly to the nuclei of the atoms of the lattice by encounters close enough to allow the exchange of momentum and energy through the action of the Coulomb fields. If a particle gives an atom more than sufficient energy to displace it from the lattice, the atom may interact with still other atoms in the lattice. It may displace other atoms or create other effects discussed in a later section. The quantitative development below was taken from Seitz and Koehler (Ref 10: 307-384).

The number of primary atoms displaced by an incident particle, having energy E, in traversing a distance dR through a solid is

$$dn = n_o \, \sigma_d \, dR_1 \tag{3}$$

where n_o is the number of atoms per unit volume and σ_d is the cross section for a collision in the Rutherford range and is given by

$$\sigma_d = \frac{Q}{E} = 4 \pi A_h \, \frac{M_1}{M_2} \, \frac{Z_1^2 \, Z_2^2 \, R_h^2}{E E_d} \tag{4}$$

where A_h is the Bohr radius for hydrogen (0.529 Å)

M_1 is the mass of the incident particle

M_2 is the mass of the target atom

Z_1 is the atomic number of the incident particle

Z_2 is the atomic number of the target atom

E is the energy of the incident particle

E_d is the energy necessary to displace an atom from the lattice.

R_h is the Rydberg energy for hydrogen (13.54 EV). The total number of primary atoms displaced would be

$$n = n_o Q \int_{R - \Delta R_1}^{R} \frac{dR}{E} \tag{5}$$

where R is the range. For a thick target, $R_1 = R$, and E is given by

$$R(E) = CE^{\gamma} \tag{6}$$

where C and γ are empirically determined constants. For deuterons between 2 and 10 MEV, $C = 2.08$ and $\gamma = 1.63$ (Ref 7:54). Since the range of protons is approximately twice the range of deuterons, γ in (6) is the same for protons and $C = 1.04$ (Ref 5:650). Evaluating (5) for a thick target

$$n = n_o R \frac{\gamma}{\gamma - 1} \sigma_d \tag{7}$$

The number of displacements per primary displacement is given empirically by (Ref 6:163)

$$N_d = \frac{Em}{Em - E_d} \left(0.766 + 0.352 \ln \frac{Em}{4 E_d}\right) \tag{8}$$

where N_d is the number of displacements per primary displacement and Em is the maximum energy that can be transferred to an atom

by a bombarding particle, and is given by

$$E_m = \frac{4 M_1 M_2}{(M_1 + M_2)^2} E \qquad (9)$$

The total number of displacements per incident particle is given by

$$N_t = n N_d \qquad (10)$$

More complicated defects than simple vacancy interstitial pairs are produced by radiation. The displaced atoms have small mean free paths, and the secondary displacements are produced in a small region. The defects tend to form clusters. Some energy is dissipated in producing lattice vibrations which cause a large, local increase of temperature or thermal spike. This causes another type of disordered region in the lattice. The effect of such regions should be different from that of single interstitials and vacancies (Ref 6:163). It can be seen that the damage is complex, and that quantitative prediction of conductivity change during radiation is poor.

Transient Effect. The basis of transient effects is the ionization caused by the passage of energetic charged particles through a crystal. Most of the energy of incident particles is dissipated in this way. A particle will not displace an atom from its lattice position, as described above, until the energy of the particle is slowed well into the KEV range by the ionization process. This ionization creates hole-electron pairs which usually recombine in

a very short time. There is experimental evidence, however, which indicates that trapping effects due to surface states created by ionization, decay very slowly (Ref 6:181). If these slow states are effected by the surface properties of the crystal as found by Longo and Wang, then one could expect a difference in the measured conductivity of dendrites and ordinary crystals during radiation (Ref 8:16).

Range

The range of the deuterons and protons used in the experiment was found by plotting the data of Rich and Madey (Ref 9:23-201). The tabulated ranges for 2 MEV protons and deuterons for beryllium, aluminum, copper, and lead are plotted versus atomic number in Figure 2. It may be seen that the relationship is linear. The ranges for germanium were obtained by entering Figure 2 with the atomic number of germanium and reading the range. The ranges are 1.75×10^{-3} cm and 2.67×10^{-3} cm for deuterons and protons, respectively.

Summary

Radiation damage in germanium causes two basic kinds of effects, permanent and transient. The permanent effects are the results of disordered regions in the crystal lattice which occur when atoms are displaced from their regular lattice sites by collisions with incident particles or by thermal spikes. Transient

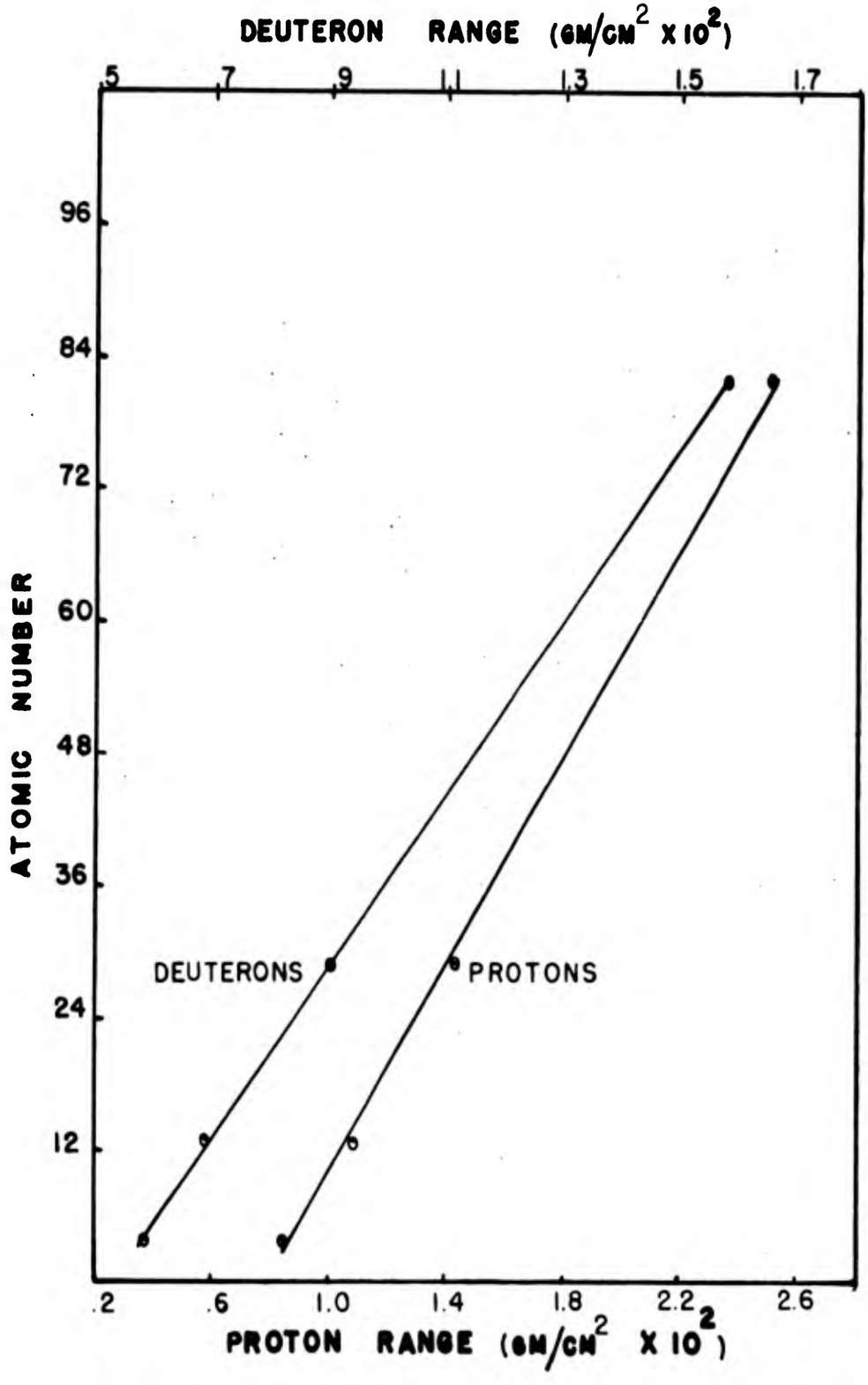

2 MEV DEUTERON AND PROTON RANGE

(FROM REF 9:23-201)

FIG. 2

effects are the result of the intense electron excitation which occurs during passage of an incident particle when its energy is still high. Both effects may change the carrier concentration in the crystal. The transient effects usually decay at a fast rate. However, experimental evidence exists which indicates that the transient effects associated with the surface states decay slowly, on the order of hours. The surface effects have also been found to be related to the surface properties of the crystal.

III. The Experiment

Crystal Preparation

The dendrite samples were cut from the same single crystal which had a very nearly constant conductivity along its length. The dendrite single crystals were manufactured by Westinghouse Corporation and made available by the Electronics Technology Laboratory. A length of single crystal of approximately 12 cm was buried in lacquer in a thick piece of glass. The lacquer was applied to protect the surface during preparation. The samples were then cut into approximately 2 cm lengths with the Electronics Technology Laboratory's Ultrasonic Cutter.

After cutting, the ends of each dendrite sample were sandblasted. The lacquer on the ends was blasted away in order to expose approximately 0.3 cm of the ends of the sample to the sand blasting operation. Next, the ends of the samples were electroplated with rhodium. The samples were dipped into a beaker of electroplating solution far enough so that the entire exposed end was plated. Following this, the lacquer was removed by dissolving it in methyl alcohol, and silver leads were soldered with indium to the electroplated ends. This process resulted in good ohmic contacts on the dendrite samples.

The ordinary P-type samples used were obtained from the Institute of Technology Physics Laboratory. When received, they

were already prepared with electroplated ohmic contacts on one surface. Silver leads were soldered with indium to these contacts. In order to facilitate mounting in the radiation apparatus and to prevent strains on the soldered connections, the samples were cemented to glass plates with epoxy resin. One N-type dendrite and one P-type ordinary crystal were cemented to each of four glass plates. P-type ordinary crystals were used because N-type ordinary crystals were not available at the time these samples were made. These samples were labeled A through D.

After the first four glass plates were prepared, the Institute of Technology Physics Laboratory made available one N-type ordinary crystal. This crystal was prepared in the same way as described for the dendrite preparation, and it was also etched with CP4. This sample was labeled H. One N-type dendrite was cut and sandblasted all along one of its smooth faces. The sandblasted face was then cemented to a copper disk with silver paste. Two thin strips were cut into a second disk, and it was placed so as to expose just part of the dendrite to radiation. This sample was used to demonstrate the possibility of making a rectifier by using a radiation process. The sample was labeled G, and a photograph of it, along with one of Sample B, is presented in Figure 3.

All of the above samples were irradiated with deuterons. After the deuteron experiments were concluded, General Instrument

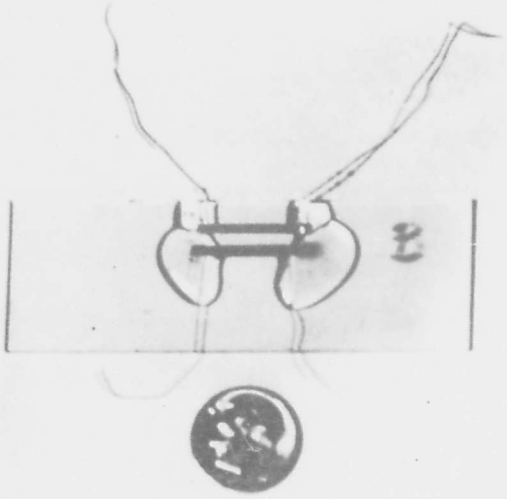

Typical Sample

Sample G

CRYSTAL SAMPLES

Fig. 3

Corporation of Woonsocket, Rhode Island, made available several N-type ordinary crystals prepared with ohmic contacts. One of these crystals, together with one N-type dendrite prepared as stated above, were cemented to a glass plate with epoxy resin. This sample was labeled E, and it was used for a proton irradiation run.

The geometry of the samples was obtained with a measuring microscope. Since two edges of a dendrite are serrated, the average of the minimums of the serrations was taken as the effective width of the dendrites. The lengths of the samples for initial conductivity calculations were the contact to contact lengths. When the epoxy resin was used to cement the crystals to the glass plates, some of the epoxy covered part of the crystal at each end of the samples. This shortened the length exposed to radiation. Table I lists the geometry of the samples along with their type, initial conductivity, and irradiating particle. The length listed is the average length exposed to radiation.

Experimental Apparatus

The Aeronautical Research Laboratories' 2 MEV Van de Graaf Accelerator was the source of radiation. A photograph of this machine appears in Figure 4. The minimum flux produced by the machine was 6.25×10^{12} particles per cm^2-sec. Since the estimated total integrated flux necessary for this experiment was on the order

Table I

Sample	Type	Initial Conductivity $(ohm\text{-}cm)^{-1}$	Irradiating Particle	Length Cm	Width Cm	Depth Cm
A-D*	N	0.672	-----**	1.64	0.117	0.029
A-O	P	0.105	-----**	1.26	0.160	0.049
B-D	N	0.661	deuteron	1.44	0.177	0.029
B-O	P	0.121	deuteron	1.26	0.152	0.064
C-D	N	0.688	deuteron	1.66	0.117	0.029
C-O	P	0.119	deuteron	1.25	0.157	0.050
D-D	N	0.655	deuteron	1.48	0.117	0.029
D-O	P	0.064	deuteron	1.26	0.174	0.060
G-D	N	***	deuteron	***	0.117	0.029
H-O	N	0.214	deuteron	0.977	0.298	0.127
E-D	N	0.665	proton	1.14	0.117	0.029
E-O	N	0.127	proton	0.578	0.299	0.025

* D-dendrite
O-ordinary

** not irradiated
*** not measured

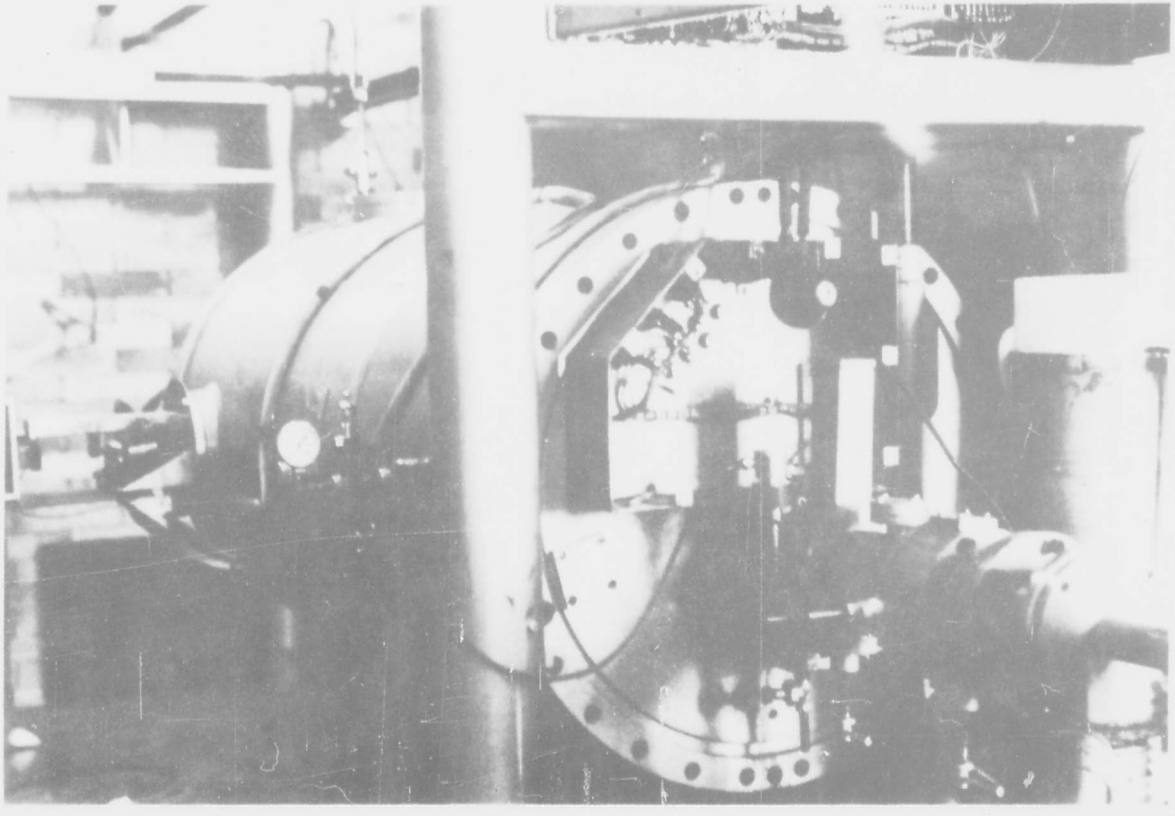

ARL VAN De GRAAF

Fig. 4

of 5×10^{11} particles per cm^2, it was necessary to reduce the flux of the machine by means of Rutherford scattering of the beam. A silver foil, 2.5×10^{-4} cm thick, was placed in a scattering chamber at the end of the drift tube as illustrated in Figure 5. Figure 6 is a schematic of the apparatus. The target sample and detector tube were placed at equal angles from the scattering foil. This made the flux at the target and at the detector a function of their distance from the foil only. The distances were 28 cm and 150 cm from the foil to the target and detector, respectively.

The detector was a silicon surface barrier type with an activation area of 50 mm^2. In order to further reduce the count rate, so as not to exceed the maximum rate of the scaling units, a tantalum shield was placed over the detector face. A hole of 0.01 cm^2 area in the shield allowed particles to strike the detector, but the count rate was reduced two orders of magnitude. The detector was connected to a Tenelec pre-amplifier through a BNC adapter at the end of the detector tube. The pre-amplifier was connected in series to an Atomic Radiation Laboratories Model 101 Linear Amplifier, a Cosmic Radiation Model 801 Multiple Coincidence Unit (used as a discriminator only), and a Berkeley Model 5510 Decimal Scaler.

The target samples were held in position in the target chamber with a pressure clip. Wires were attached to the silver

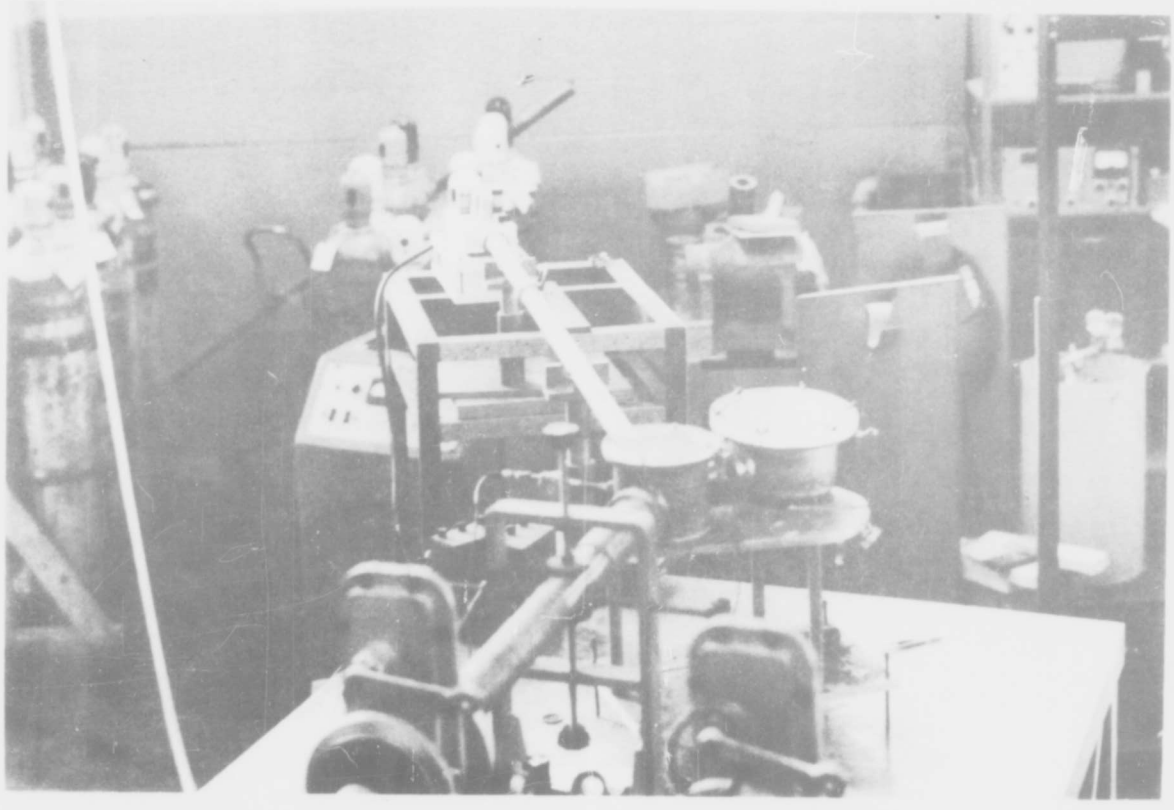

IRRADIATION APPARATUS

Fig. 5a

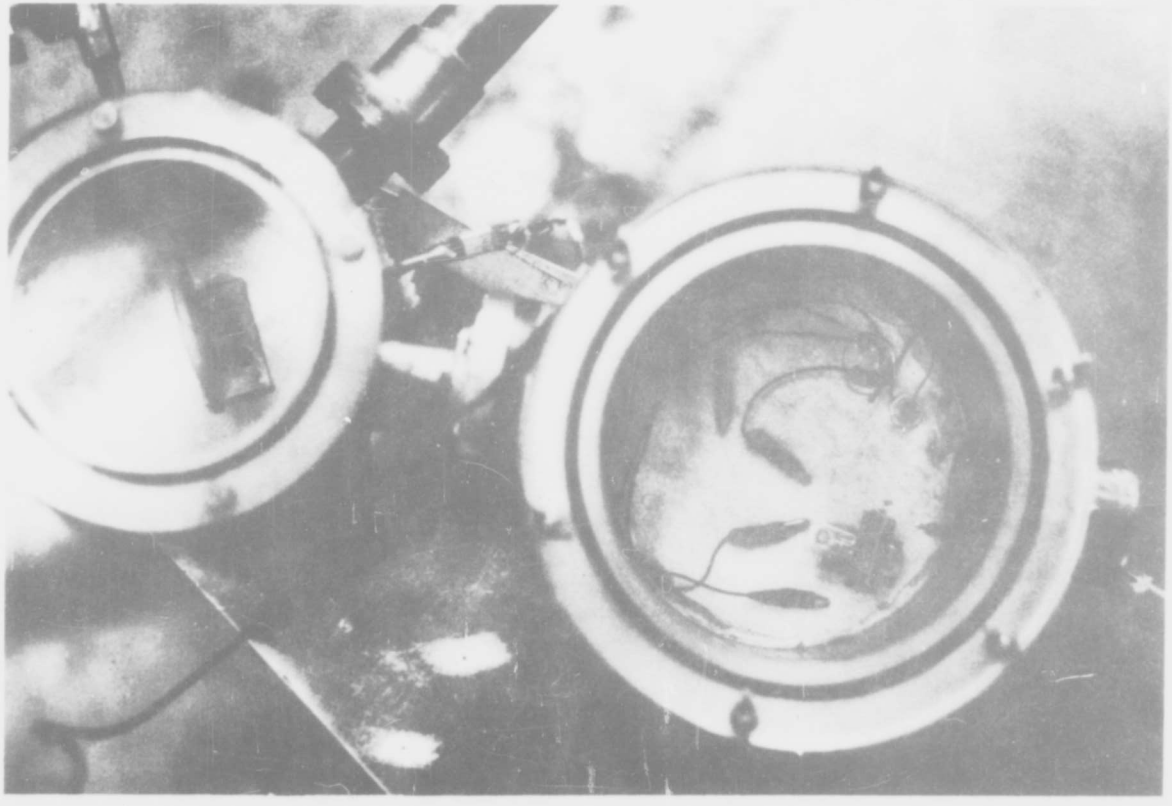

TARGET CHAMBER

Fig. 5b

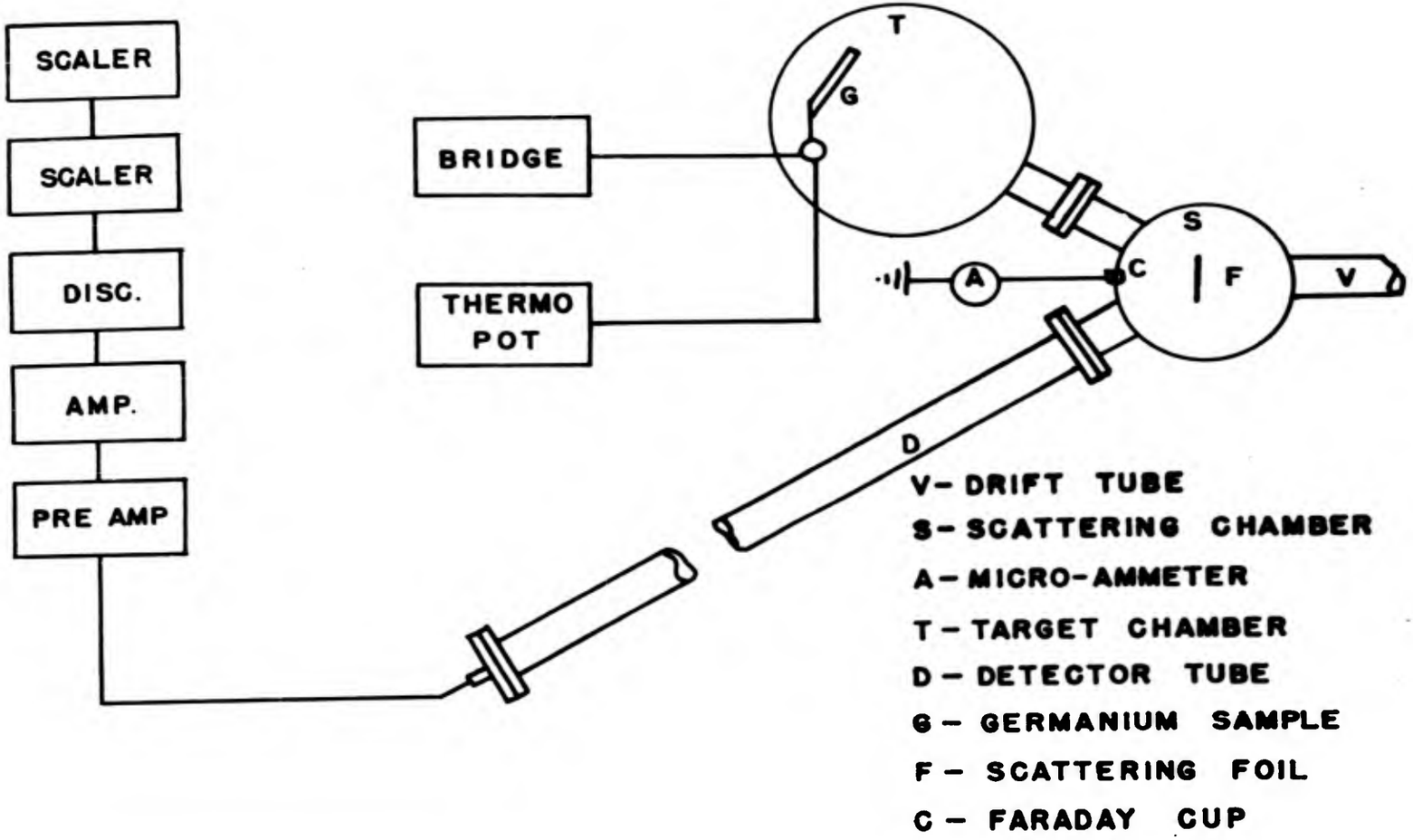

SCHEMATIC DIAGRAM OF IRRADIATION CHAMBERS AND COUNTING EQUIPMENT

FIG. 6

leads of each crystal with spring clips. These wires led outside the target chamber, through a fitting to a Model 4725 Leeds and Northrup Wheatstone Bridge. Sample resistance at various levels of flux was measured with the bridge. A copper-constantan thermocouple was taped to the glass plate of each sample. The thermocouple leads were connected to a BNC fitting in the bottom of the target chamber. Shielded wire led from the BNC fitting to a Leeds and Northrup Thermocouple Potentiometer, Model 8657C.

The conductivity type of each crystal was checked before and after irradiation with a hot probe. The probe was made in the Electronics Technology Laboratory. It was connected to a Kaylab Micro-Ammeter, Model 203, in order to read the direction of current generated when the hot probe was put in contact with the crystal.

Calibration

The equation which describes Rutherford scattering is

$$N(\theta) = \frac{N_i n_o t_f}{4 r^2} \left(\frac{e^2}{4\pi\epsilon_o} \right)^2 \frac{Z^2}{E \sin^4 \frac{\theta}{2}} \qquad (11)$$

where $N(\theta)$ is the number of particles per unit area scattered at angle θ

N_i is the number of particles striking the foil

n_o is the number of foil atoms per unit volume

t_f is the foil thickness

r is the distance from the foil

e is the electron charge

e_o is the permittivity of free space

Z is the atomic number of the foil

E is the energy of the particle

θ is the angle of scatter.

In the apparatus described above the angle of scatter, θ, was equal for both target and detector tube. It can be seen from (11) that

$$\frac{N(\theta)_t}{N(\theta)_d} = \frac{r_d^2}{r_t^2} \tag{12}$$

where $N(\theta)_t$ is the number of particles per unit area striking the target

$N(\theta)_d$ is the number of particles per unit area striking the detector

r_d is the distance from the foil to the detector

r_t is the distance from the foil to the target.

A value of 28.6 was obtained when (12) was evaluated for the distances in the apparatus.

In order to calibrate the apparatus a second silicon detector and counting circuit was installed. The second detector was placed in the target chamber in the same position a sample would be placed during the experiment. A second tantalum shield with the same size

hole was placed over the second detector face. Five minute runs were made at beam currents of 0.1 to 5 micro-amps. The beam current was read on the micro-ammeter in the Faraday Cage Circuit. The Faraday Cage was located directly behind the silver foil in the scattering chamber (see Figure 6). At the end of each five minute run, both scaler readings were recorded.

A correction was made to the scaler readings for counting losses due to the finite resolving time of the circuits at low count rates; the counting systems were nonparalyzable, and the true number of counts per unit time was given by (Ref 5:787)

$$N_C = \frac{n_C}{1 - n_C \rho} \tag{13}$$

where, here N_C is the true number of counts per unit time

n_C is the observed number of counts per unit time

ρ is the resolving time of the circuit.

Now

$$\Phi = N_C t \tag{14}$$

where Φ is the true total number of counts in the time of radiation, t.

Also

$$n_C = \frac{\phi}{t} \tag{15}$$

where ϕ is the observed total counts in time t.

Therefore

$$N_c = \frac{\frac{\phi}{t}}{1 - \frac{\phi}{t}\rho} \tag{16}$$

and

$$\Phi = \frac{\phi}{1 - n_c \rho} \tag{17}$$

Since the areas of the detectors exposed to radiation are equal,

$$\frac{\Phi_t / A_t}{\Phi_d / A_d} = \frac{\Phi_t}{\Phi_d} = \frac{\phi_t \ (1 - n_{cd} \rho)}{\phi_d \ (1 - n_{ct} \rho)} \tag{18}$$

where the subscripts t and d refer to target and detector, respectively, and it was assumed that

$$\rho_t = \rho_d$$

Equation (18) was solved by an iteration process. A value of ρ was assumed, and for each run at a particular beam current the ratio Φ_t / Φ_d was calculated. This process was repeated until the differences between the ratios calculated at each beam current were a minimum. The value of ρ was found to be 4.46×10^{-6} seconds. The ratio Φ_t / Φ_d versus n_t is plotted in Figure 7 for deuterons and protons. The values of 25.8 and 22 were taken as the values of Φ_t / Φ_d for deuterons and protons, respectively. Figure 7 also indicates the maximum value of n_c possible for the detectors used. During the experiments the count rate was held at a fairly constant value between 3.5×10^4 and 4.2×10^4 particles per second.

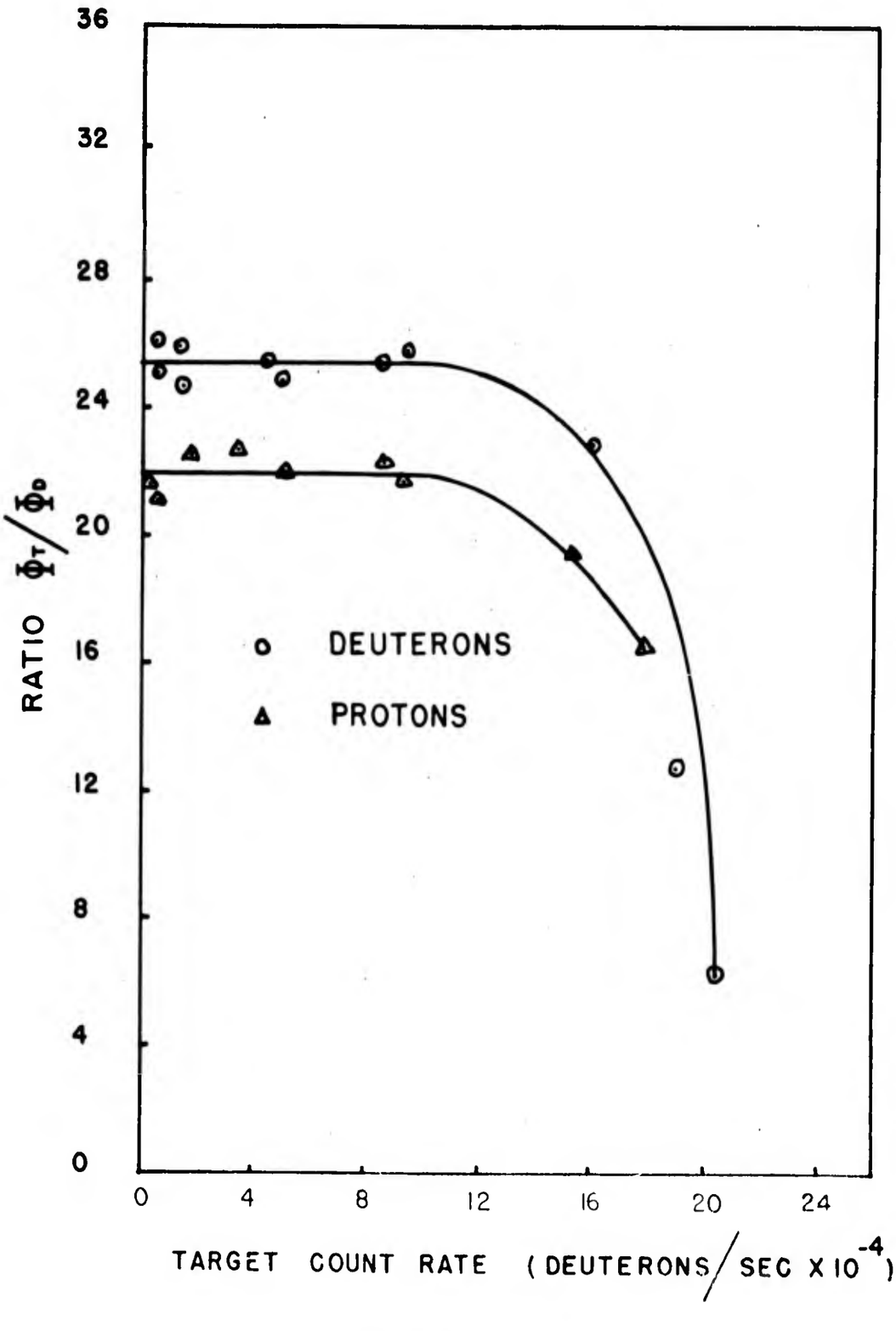

CALIBRATION CURVES

FIG. 7

The measured values of Φ_t / Φ_d of 25.8 for deuterons and 22 for protons are less than 28.6, the value calculated from (12). This indicates a reflection of particles from the detector tube walls. As might be expected, the reflection was greater with the lighter protons.

Since the areas which admitted particles to the detectors was 0.01 cm^2, and the ratio, Φ_t / Φ_d, was found to be 25.5 for deuterons and 22 for protons, it can be seen for the case of deuterons that

$$\frac{\Phi_t}{A} = \frac{25.5\ \Phi_d}{A} \tag{20}$$

where

$$A = A_t = A_d \tag{21}$$

It was possible to multiply Φ_d by a constant to obtain a value for the total integrated deuteron flux. Φ_d was obtained from (17). The same held true for the experiment with protons.

Experimental Procedure

The conductivity type of each sample was checked before irradiation was started with the hot probe. At the same time the sample was placed in the target chamber, a shield was placed over the entrance to the chamber. The Van de Graaf was then started and adjusted to a beam current reading near 5 micro-amps. The counting circuit was then checked for proper operation, and the

count rate was checked to make sure it was in the linear portion of Figure 7. At this point, irradiation was stopped, and the shield was removed from the entrance to the target chamber.

Next, the irradiation was resumed and stopped at intervals of 50 seconds. While the irradiation was stopped, the scaler, bridge, and thermocouple potentiometer readings were recorded. The intervals of irradiation were lengthened to 100, 500, 1000, and 1500 seconds as the change in resistance slowed down. The readings were recorded and irradiation resumed in approximately three minutes. Each run took around seven hours to complete. The proceedure for each run was the same with the exception of sample G, which was irradiated to a level of 1.85×10^{12} deuterons per cm^2 without interruption. At the conclusion of each run, the conductivity type of the samples was checked again with the hot probe.

IV. Results

The range of the deuterons and protons was small compared to the depth of the crystals. Therefore, the damage done to the crystals was not homogenous, but a function of depth. During irradiation, the crystals consisted of a large undamaged layer with a constant conductivity, and a small damaged layer with quite a different varying conductivity. However, the admittances of the two parts were additive in this geometry. Each crystal was analyzed as two resistances in parallel. Thus

$$Y_t = Y_i + Y_c \tag{22}$$

where Y_t is the total admittance of the crystal

Y_i is the admittance of the irradiated part

Y_c is the admittance of the constant part.

And

$$\Delta Y_t = \Delta Y_i \tag{23}$$

since Y_c is constant. The initial conductivity is given by

$$\sigma = \frac{L}{wd} Y \tag{24}$$

where L, w, and d are the length, width, and depth of the unirradiated crystal. The change in conductivity during radiation is

$$\Delta \sigma_i = \frac{L}{wR} \Delta Y_t \tag{25}$$

where $\Delta \sigma_i$ is the change in the conductivity of the irradiated part of the crystal and R is the particle range. From (1) for an N-type

crystal

$$\Delta\sigma_i = e\mu_e \Delta n_e \tag{26}$$

Equating (25) and (26) and solving for Δn_e

$$\Delta n_e = \frac{L}{wR} \frac{\Delta Y_t}{e\mu_e} \tag{27}$$

Dividing (27) by the change in integrated particle flux, ΔNVT, we get

$$\frac{\Delta n_e}{\Delta NVT} = \frac{L}{wRe\mu_e} \frac{\Delta Y_t}{\Delta NVT} \tag{28}$$

In order to get the number of electrons removed per incident particle, the numerator of (28) must be multiplied by the irradiated volume, LwR, and the denominator must be multiplied by the irradiated area, Lw. This is true because Δn_e is the change in the number of conduction electrons per unit volume, and ΔNVT is in particles per cm^2. Performing this operation and cancelling like terms

$$\frac{\Delta C_e}{\Delta \Phi} = \frac{L}{we\mu_e} \frac{\Delta Y_t}{\Delta NVT} \tag{29}$$

where $\Delta C_e / \Delta\Phi$ is the number of carriers (electrons) removed per incident particle. A similar argument can be made for the hole injection rate in an irradiated P-type crystal. It may be seen that (29) is independent of the particle range. A comparison of the parameter, $\Delta C / \Delta\Phi$, shows the difference in radiation damage for two crystals quite clearly.

The results of the experiment are in general agreement with earlier radiation experiments reported in the literature. The

conductivity of the N-type samples, first decreased and then increased, while the conductivity of the P-type samples increased from the beginning. The conductivity type of the N-type samples changed to P-type during irradiation. These general effects were expected. The goal of the experiment was to compare the differences of the rates of change of carriers in the dendrite and ordinary N-type crystals. The P-type crystals were irradiated to demonstrate the validity of the experimental apparatus and proceedures. Figure 8 through 12 are plots of measured admittance versus measured integrated deuteron and proton flux. Figures 8, 9, and 10 are for an N-type dendrite, an N-type ordinary, and a P-type ordinary crystal, respectively. Deuterons were the irradiating particles. Figures 11 and 12 are for an N-type dendrite and an N-type ordinary crystal, respectively. Here protons were the irradiating particles. Since admittance is proportional to conductivity, Figures 8 through 12 show that the experiment was in general agreement with earlier experiments, such as that done by Brattain and Pearson (Ref 3:846-850).

Most displaced atoms in the germanium lattice occur near the end of the bombarding particle's range (Ref 3:849). The volume near the end of the range changes to P-type first, and the rest of the irradiated part follows at a later time. The maximum change in conductivity would be the change from the measured initial value to the value of intrinsic germanium at room temperature. If we let this change be $\Delta\sigma$ max, then

$$R > \frac{L}{w} \frac{\Delta Y_t}{\Delta \sigma \max} \tag{30}$$

where ΔY_t was determined from the initial and minimum values of Figures 8 through 12. Equation (30) would be an equality if the damage done in the irradiated part of the crystal was homogenous. Since this was not the case, the value computed for $\Delta \sigma$ max was too large in each case. Therefore, (30) must be an inequality.

Equations (29) and (30) were evaluated for each sample, and those values are listed in Table II along with the calculated values of N_d and N_t from equations (8) and (10). The result of two earlier experiments with N-type ordinary crystals of germanium are listed for comparison. No results were obtained for samples A and B. The contacts went bad on A, and the counting circuit malfunctioned during the irradiation of B.

Current measurements at various voltages were made on sample G. A probe was placed in contact with the surface of the crystal in both the irradiated and shielded areas. The copper plate was the other contact to the crystal, therefore, the electric field was perpendicular to the crystal's smooth face. These measurements were made thirty days after the crystal had been exposed to radiation. It was assumed that the transient effects had disappeared, and that the healing effects at room temperature were

Table II

Sample	Particle and energy in MEV		Conductivity Type	$\frac{\Delta C_e}{\Delta \Phi}$	$\frac{\Delta C_h}{\Delta \Phi}$	N_t	N_d	Range from data cm x 10^3
(Ref 6:162)	α	4.5	N	180	---	87	3.7	---
(Ref 3:849)	α	5.3	N	78	8.6	59	---	> 1.83
C-D*	d	2	N	14	0.63	20	3.4	> 0.375
D-D	d	2	N	13	0.72	20	3.4	> 0.426
H-O	d	2	N	6.9	1.3	20	3.4	> 1.08
C-O	d	2	P	--	2.4	20	3.4	--
D-O	d	2	P	--	2.8	20	3.4	--
E-D	p	2	N	3.6	0.18	14	3.1	> 0.358
E-O	p	2	N	2.2	0.10	14	3.1	> 1.05

$\frac{\Delta C_e}{\Delta \Phi}$ electrons removed per incident particle

$\frac{\Delta C_h}{\Delta \Phi}$ holes induced per incident particle

N_t calculated displacements per incident particle

N_d calculated number of displacements per primary

* D-dendrite, O-ordinary

-- not applicable

--- not reported

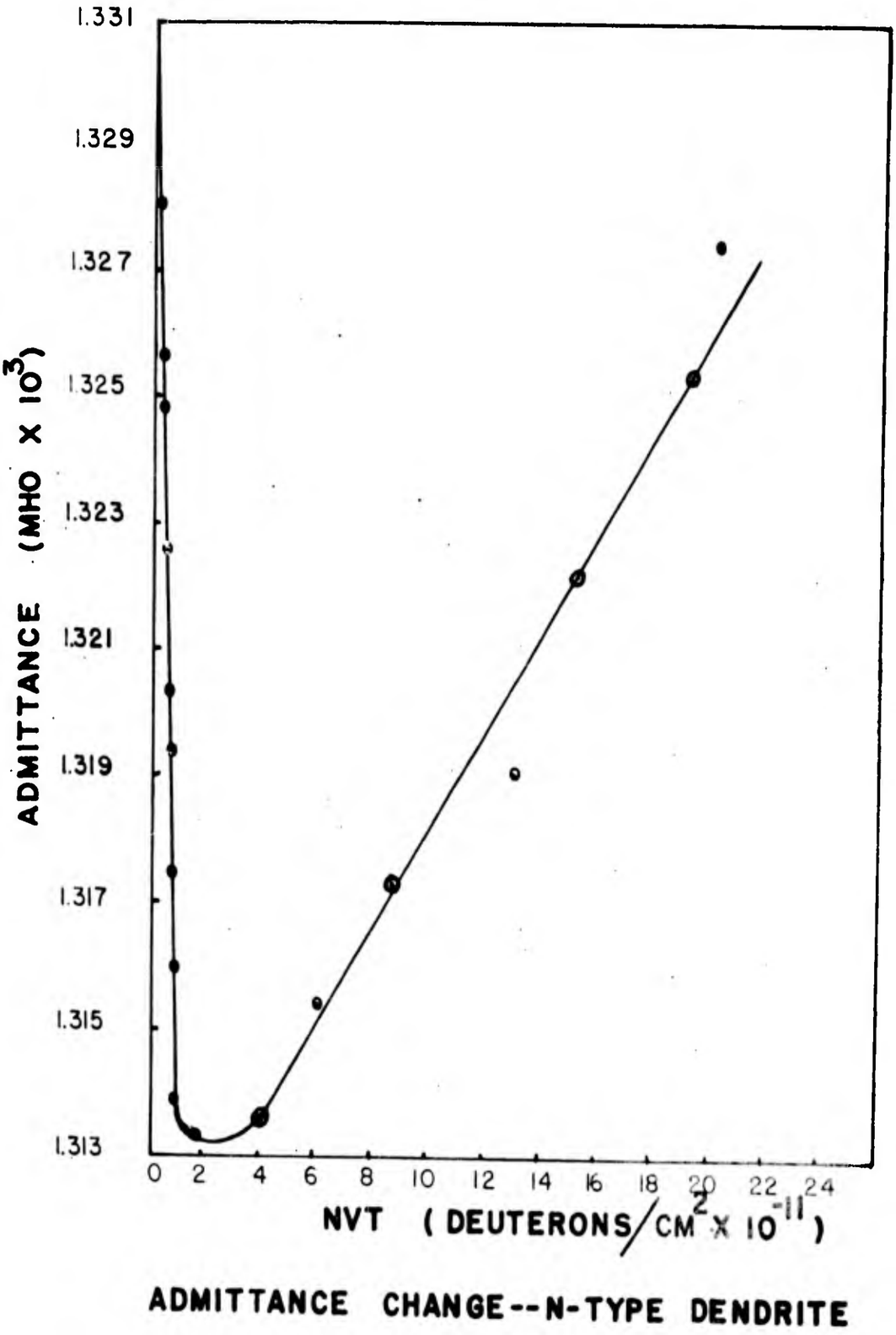
1.331
1.329
1.327
1.325
1.323
1.321
1.319
1.317
1.315
1.313
ADMITTANCE (MHO X 10^3)
0 2 4 6 8 10 12 14 16 18 20 22 24
NVT (DEUTERONS/CM^2 X 10^{-11})
ADMITTANCE CHANGE--N-TYPE DENDRITE

FIG. 8

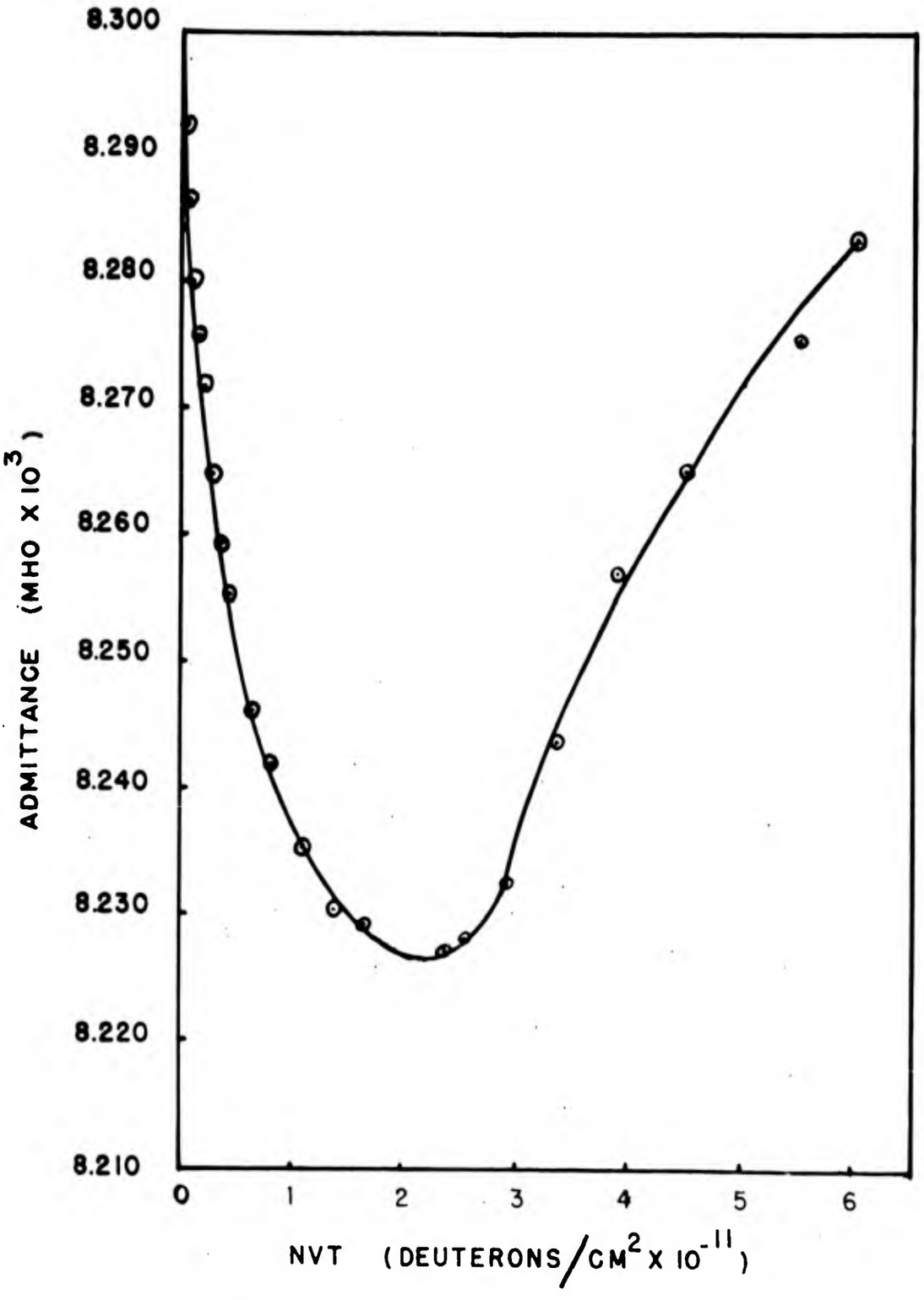

ADMITTANCE CHANGE -- N-TYPE ORDINARY

FIG. 9

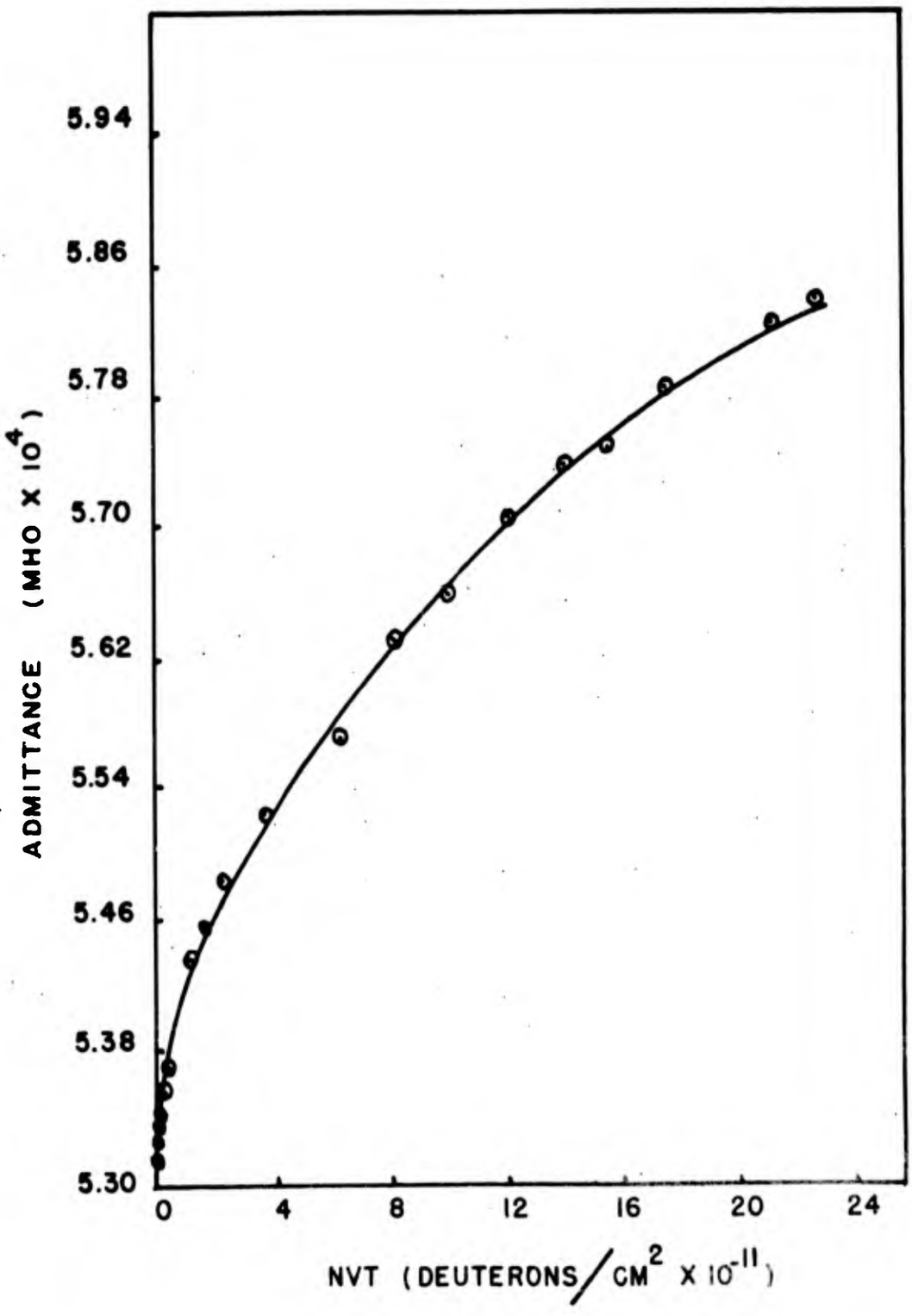

ADMITTANCE CHANGE -- P-TYPE ORDINARY

FIG. 10

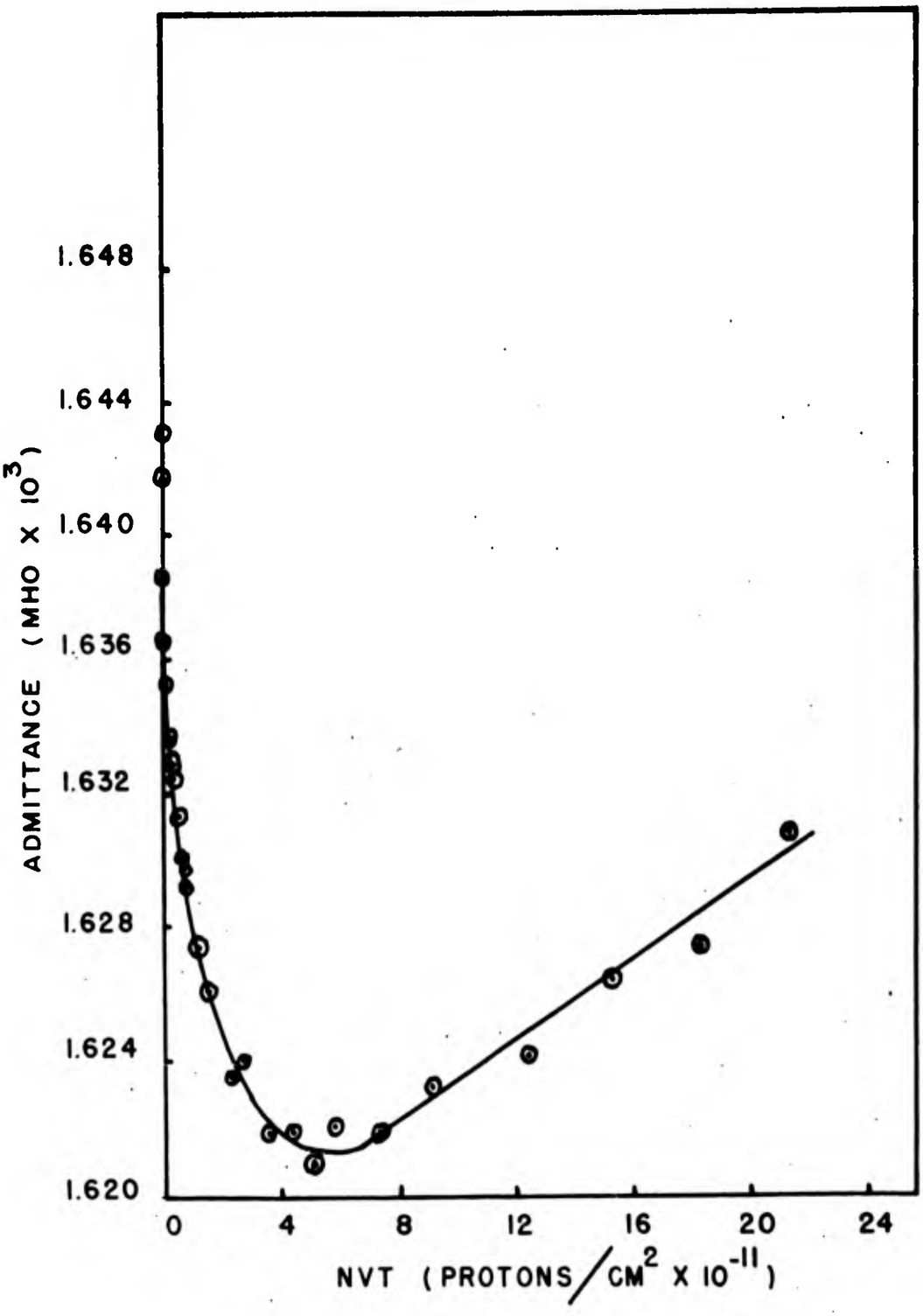

ADMITTANCE CHANGE -- N-TYPE DENDRITE

FIG. 11

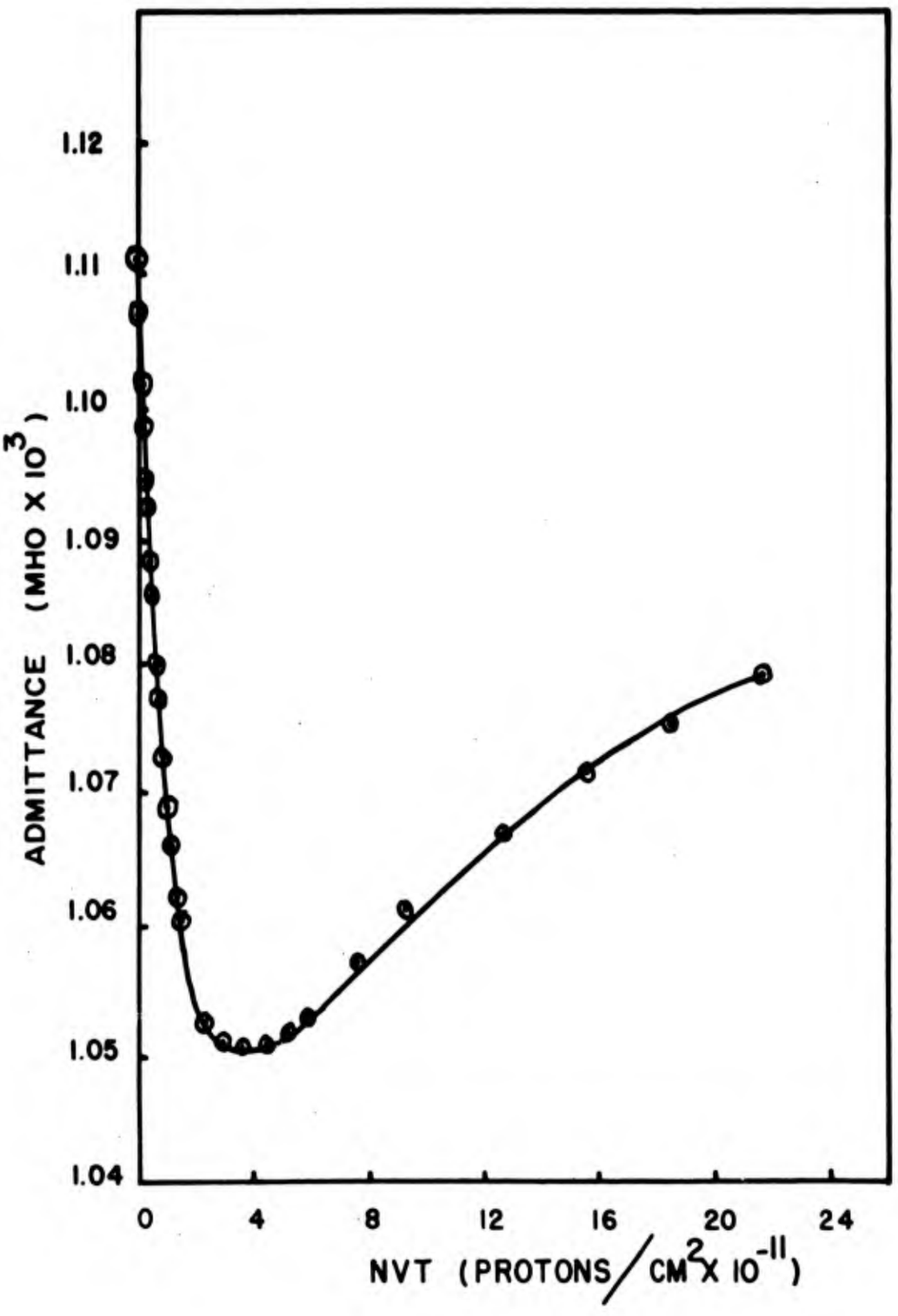

ADMITTANCE CHANGE -- N-TYPE ORDINARY

FIG. 12

complete at this time. The probe used formed a rectifying contact with the crystal. However, the effect of the P-N junction formed by irradiation was clear. These measurements are presented in Figure 13.

The thermocouple potentiometer readings indicated the temperature remained in a range of $1^{o}C$ for all runs. This indication was in doubt, however, and the reasons for the uncertainty will be discussed in the next chapter.

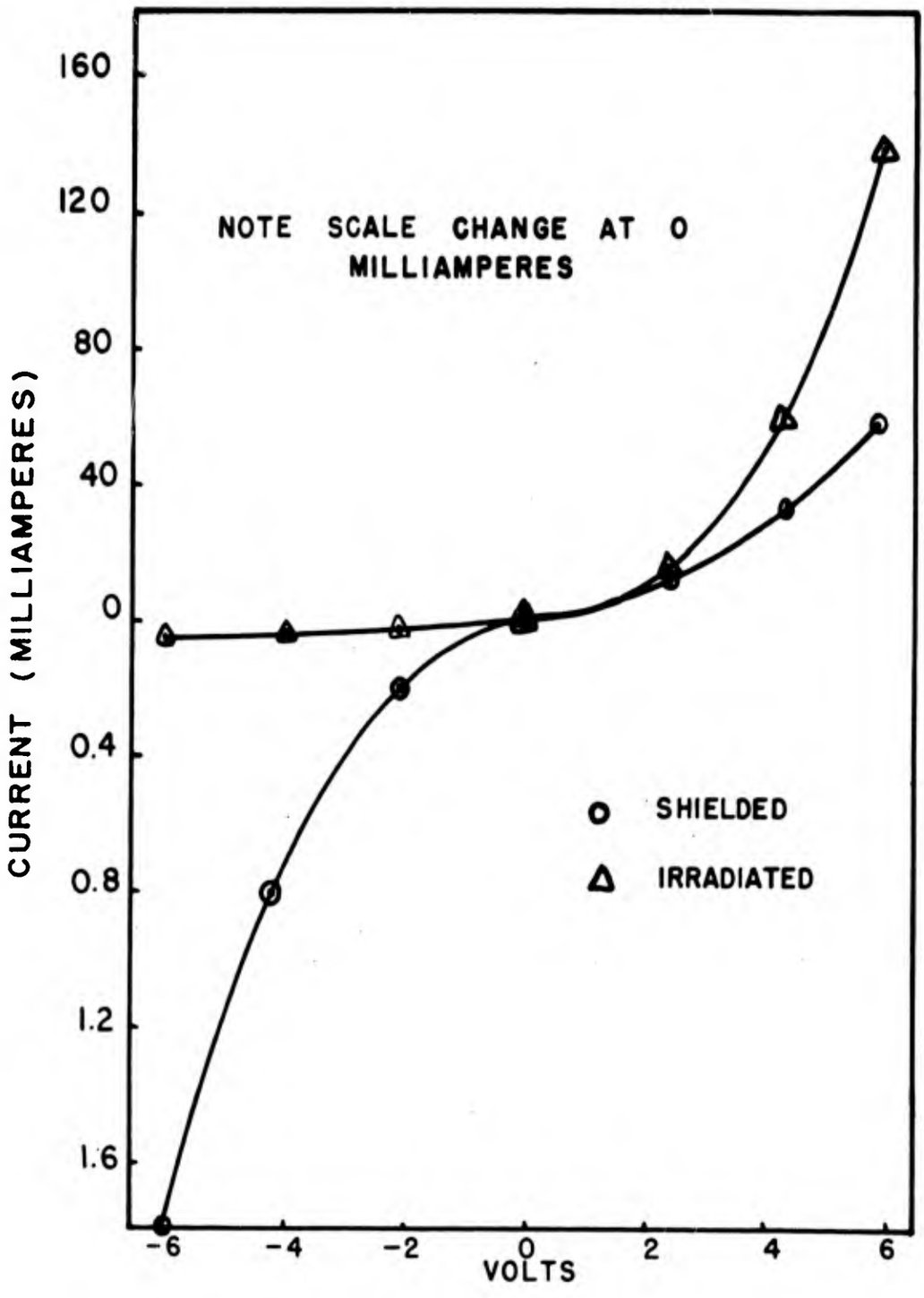

RECTIFIER EFFECT- SAMPLE G

FIG. 13

V. Conclusions

The changes in conductivity of the irradiated crystals were in general agreement with experiments reported in the literature. As stated before, the conductivity of all N-type crystals first decreased and then increased at a slower rate. Conductivity in the P-type crystal increased from the beginning of radiation. The N-type crystals changed to P-type during radiation.

As indicated in Table II, the number of carriers removed per incident deuteron was greater in the dendrite by a factor of approximately 2. The factor was 1.6 greater for the crystals irradiated with protons. These results could be explained by the introduction of acceptor states associated with the surface into the energy gap. Longo and Wang have reported differences in the conductivity after irradiation of silicon crystals which had different surface preparation (Ref 8:16). They proposed slow surface states which were introduced during irradiation with charged particles. These states, acting as hole traps, explained an excess conductivity after ultra-violet illumination. The excess conductivity decayed very slowly. The results of the present report could be explained by the introduction of surface states caused by irradiation. The states would differ from those proposed by Longo and Wang. They would have to be acceptor states acting as electron traps, and be more numerous in the more perfect surfaces of the dendrites.

Table II also shows that the hole production rate was greater by a factor of 1.8 in the dendrite during proton irradiation. The deuteron irradiation experiments, however, showed that hole production was greater in the ordinary crystal by a factor of 2. This discrepancy could be explained by the heating of sample H, the ordinary N-type crystal used for deuteron irradiation. This sample was approximately five times as thick as the other samples, and it, therefore, contained more germanium that was not affected by irradiation. All of sample H, however, was affected by temperature changes that occured during the run. Thus, the effects of temperature change would be greater in this crystal than any of the others.

It is believed that the temperature increased a few degrees in each sample during its irradiation. The thermocouple did not indicate this increase, but it was taped to the glass plates approximately 1.5 cm from the crystals. This arrangement would indicate only large temperature variations. A temperature increase of a few degrees would have a much greater effect in sample H than the other samples because of its greater unirradiated volume. The temperature increase would in turn cause an increase in conductivity which would appear as a greater measured value of ΔY_t in equation (29). The result would be a value for the hole production rate in this sample which is too large. It is believed that this effect was

large enough to invalidate the data presented in Figure 9 after the minimum conductivity point had been reached. Assuming this is true, the difference in the hole production rate between the dendrites and ordinary crystals could also be explained by introduction of acceptor states associated with the surface. These states would have to produce holes after all the conduction electrons were removed.

The conductivity of the P-type samples steadily increased from the beginning of irradiation as expected. Figure 10 shows the increase was not linear. It is believed this effect was caused by the P-type material approaching the point where further irradiation has no effect on the conductivity (Ref 6:168). For this reason the hole production rates for the two P-type samples were taken from the first few data points where the relationship is essentially linear.

The ranges of the particles presented in Table II, which were found by evaluating (30), are less than those found from Figure 2. This indicates non-homogeneous damage in all the samples. However, the ranges found from (30) for dendrites were less than those for ordinary crystals by a factor of 3. This indicates more homogeneous damage in the ordinary crystals. If many acceptor states are introduced on the surface of a dendrite, there would be more damage done both on the surface and near the end of the particle range than would be done in the region between them. This would

result in less homogeneous damage than in the ordinary crystals. It would also cause the calculated ranges to be less. Therefore, these calculated ranges also support the theory of surface states caused by radiation damage which are relatively more important on the surfaces of the dendrites.

The results presented in Figure 13 demonstrate the possibility of making electronic devices using only a radiation process. Even though the probe used on sample G made a rectifying contact with the surface, the effect of the P-N junction formed in the irradiated areas is clear. The conductivity can be controlled by the amount of radiation, and the depth of the P-N junction can be controlled by the energy of the bombarding particle. Since the lifetime is an important parameter in solid state electronic devices, more information would be necessary on lifetime change with radiation before the possibility of making such a device this way becomes a certainty. Suggestions for measuring lifetime in a later experiment are contained in the appendix. The ease of manufacturing such devices in this manner should certainly provide motivation for further investigation.

Bibliography

1. Bennett, A.I., and R.L. Longini. "Dendritic Growth of Germanium Crystals." Physical Review, 116:53-61 (October 1959).

2. Blount, E.I. "Energy Levels in Irradiated Germanium." Journal of Applied Physics, 30:1218-1221 (August 1959).

3. Brattain, W.H., and G.L. Pearson. "Changes in Conductivity of Germanium Induced by Alpha-Particle Bombardment." Physical Review, 80:846-850 (December 1959).

4. BrockDale, E., et al. Investigations and Measurements of Properties of Single-Crystal Silicon. ASTIA Document No. AD117072. Washington: GPO, (May 1957).

5. Evans, R.O. The Atomic Nucleus. New York: McGraw-Hill Book Company, Inc., 1955.

6. Fan, H.Y., and K. Lark-Horovitz. "Irradiation Effects in Semiconductors," in Effects of Radiation on Materials, edited by J.J. Harwood, et al. New York: Reinhold Publishing Company, 1958.

7. Lark-Horovitz, K. "Nucleon-bombarded Semi-conductors." in Semi-conducting Materials, edited by R.W. Ditchburn. New York: Academic Press Inc., 1951.

8. Loferski, J.J., et al. Proceedings of the Second Conference on Nuclear Radiation Effects on Semiconductor Devices, Materials and Circuits, edited by S.L. Marshall and O. Fisch. New York: Cowan Publishing Corp., 1959.

9. Rich, M., and Madey, R. Range Energy Tables. UCRL-2301. Washington:GPO, 1954.

10. Seitz, F., and J.S. Koehler. "Displacements of Atoms During Irradiation," in Solid State Physics, Vol II, edited by F. Seitz and D. Turnbull. New York: Academic Press Inc., 1956.

11. Shockley, W. Electrons and Holes in Semiconductors. New York: D. Van Nostrand Company, Inc., 1950.

Appendix

Suggestions for Lifetime Measurements

Lifetime measurements during radiation were attempted as part of this investigation. They were unsuccessful because of a faulty Kerr cell in the Baird Lifetime Measuring Kit. The light pulse, as measured with a photo-tube, had a decay constant of 35 micro-seconds. All the samples used in the experiment also indicated a lifetime of 35 micro-seconds when measured with the kit. Apparently, the samples actually had a faster lifetime, and the measurements on the samples only indicated the characteristic of the light.

BrockDale, et al, in their investigation of lifetime measuring techniques, have suggested an apparatus and a circuit for lifetime measurements that would be easy to build and operate (Ref 4:17-21). The optical and electric schematic diagrams for this apparatus are presented in Figures 14 and 15, respectively.

The light source, a tungston lamp, is interrupted by the rotating disk. The disk drive is a small 110 volt series-wound grinder motor which turns the disk at about 10,000 RPM.

The process of photographing the oscilloscope trace of the decay and replotting it on logarithmic paper has been avoided by matching the decay of the photoconductivity against the decay of current in an R-C circuit. The two decay curves are subtracted

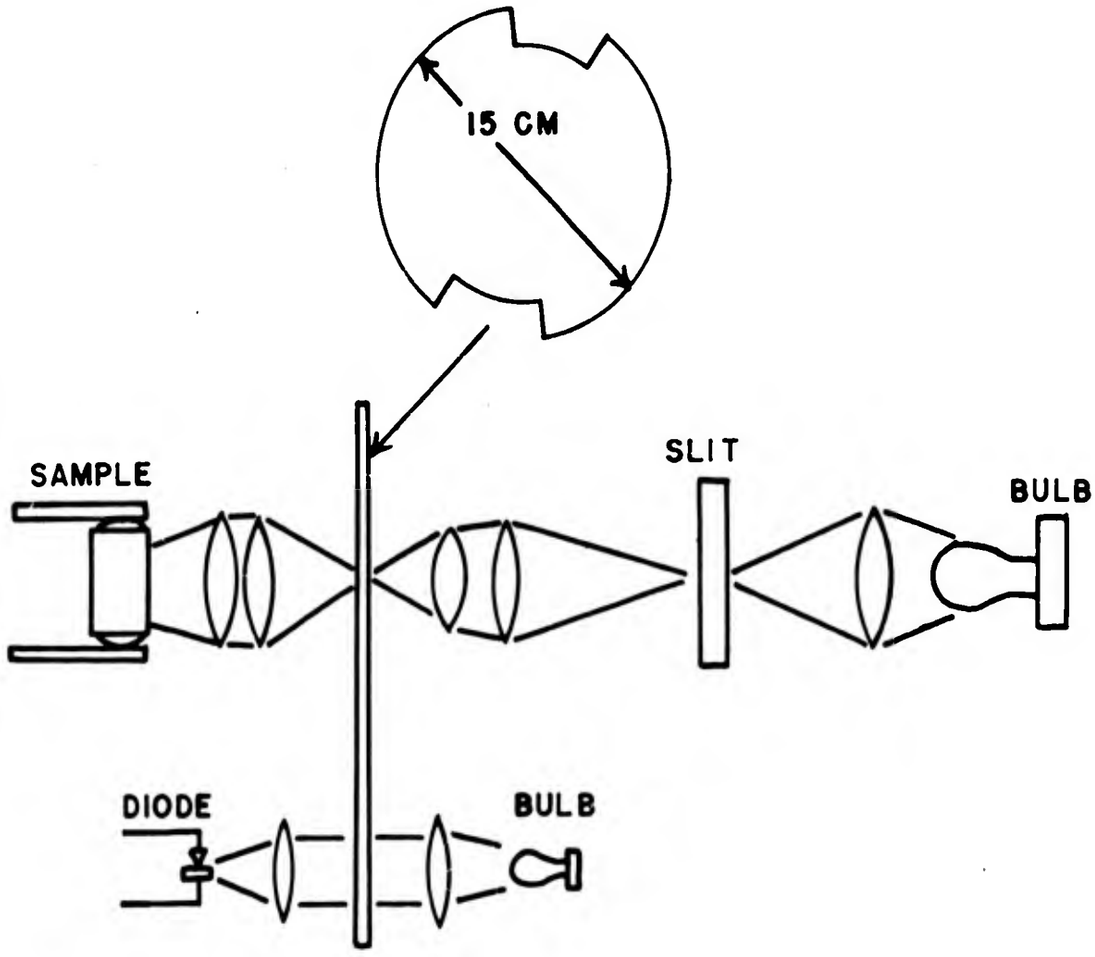

OPTICAL SCHEMATIC

(FROM REF. 4:20)

FIG. 14

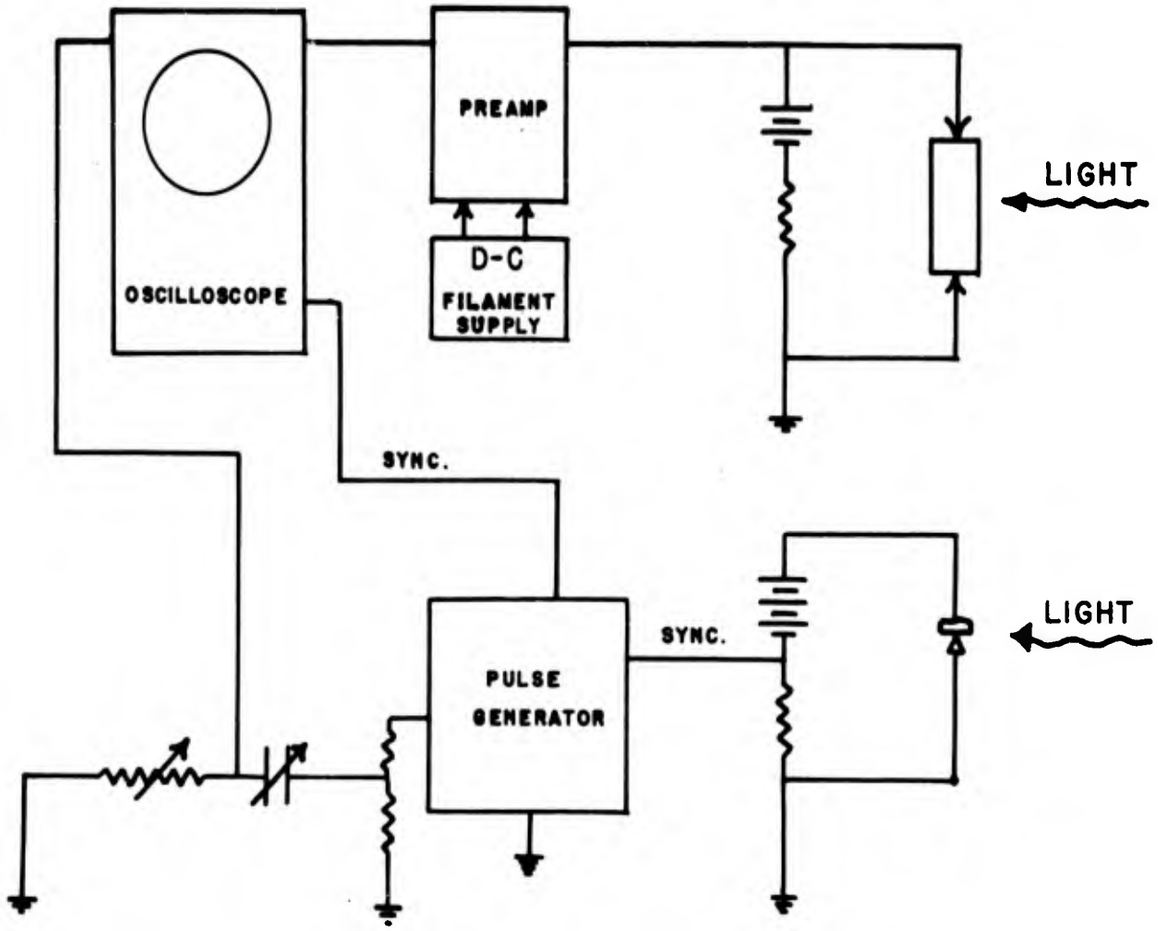

ELECTRIC SCHEMATIC

(FROM REF 4:20)

FIG. 15

in the differential amplifier of the oscilloscope so that when the two curves are identical, the oscilloscope trace is a horizontal straight line.

The pulse generator is triggered by the signal from an illuminated germanium P-N junction diode. The light source for the trigger is separate from that for the photoconductivity measurements, but the light is interrupted by the same disk. The variably delayed sweep on the oscilloscope and the trigger delay in the pulse generator provide the necessary versatility for synchronizing the two signals and observing any desired part of the decay.

GA/Phys/62-9

Vita

Ralph Henry Jacobson was born on [redacted] in [redacted], the son of Claude Quaile and Gertrude Mary Jacobson. Upon graduation from Davis High School in Kaysville, Utah, he entered the University of Utah. He was admitted to the United States Naval Academy in 1952. After graduation in 1956, he was commissioned in the United States Air Force. His military assignment prior to coming to the Institute of Technology was as a tactical pilot in the 464th Troop Carrier Wing of the Tactical Air Command.

Permanent Address: [redacted]

This Thesis was typed by Mrs. Jack E. Hesse, Jr.

UNCLASSIFIED